



Glial cholesterol redistribution in hypoxic injury *in vitro* influences oligodendrocyte maturation and myelination



Vadanya Shrivastava ^a, Sagar Tyagi ^a, Devanjan Dey ^a, Archna Singh ^a, Jayanth Kumar Palanichamy ^a, Subrata Sinha ^a, J.B. Sharma ^b, Pankaj Seth ^c, Sudip Sen ^{a,*}

^a Department of Biochemistry, All India Institute of Medical Sciences, New Delhi, India

^b Department of Obstetrics and Gynecology, All India Institute of Medical Sciences, New Delhi, India

^c Department of Molecular and Cellular Neuroscience, National Brain Research Centre, Manesar, Haryana, India

ARTICLE INFO

Keywords:

Astrocytes

Oligodendrocytes

Cholesterol

Hypoxia

Oligodendrocyte maturation

ABSTRACT

Hypoxic insult to the fetal brain causes loss of vulnerable premyelinating oligodendrocytes and arrested oligodendrocyte differentiation. Astrocytes influence oligodendrocyte differentiation and the astrocytic response to hypoxia could affect oligodendrocyte maturation under hypoxia. To identify pathways by which astrocytes influence oligodendroglial maturation in hypoxic injury, human fetal neural stem cell-derived astrocytes were exposed to 0.2 % oxygen for 48 hours. Transcriptomic analysis revealed the upregulation of the cholesterol-biosynthesis pathway in hypoxia-exposed astrocytes. Hypoxia-exposed primary astrocytes and astrocytic cell line (SVG) showed increased expression of hydroxy-methyl-glutaryl-CoA reductase (HMGCR), squalene epoxidase (SQLE), apolipoprotein E (apoE) and ATP-binding cassette transporter 1 (ABCA1) on qPCR and Western blot. Hypoxic SVG also showed increased cholesterol content in cells and culture supernatants and increased cell surface expression of ABCA1. Interestingly hypoxia-exposed premyelinating oligodendrocytes (Mo3.13) showed reduced cholesterol along with decreased expression of HMGCR and SQLE on qPCR and Western blot. Exogenous cholesterol increased the differentiation of Mo3.13 as measured by increased expression of myelin basic protein (MBP) on flow cytometry. Hypoxia exposure resulted in increased cholesterol transport from astrocytes to oligodendrocytes in cocultures with BODIPY-cholesterol labelled SVG and membrane-labelled Mo3.13. As exogenous cholesterol enhanced oligodendrocyte differentiation, our findings indicate that increased cholesterol synthesis by astrocytes and transport to oligodendrocytes could supplement oligodendroglial maturation in conditions of hypoxic brain injury in neonates.

1. Introduction

Hypoxic injury to the developing fetal brain can result in widespread neuronal loss and demyelination leading to long-term cognitive and neuromotor deficits. Oligodendrocytes, the myelin producing cells in the central nervous system differentiate from fetal neural stem cells (FNSCs) through the intermediate stages of proliferative oligodendrocyte precursor cells (OPCs) and post-mitotic migratory premyelinating oligodendrocytes [1]. Loss of myelination seen in hypoxic-ischemic brain injury occurs secondary to injury to vulnerable premyelinating oligodendrocyte population in the preterm fetal brain [2].

Astrocytes are glial cells that have numerous important roles in maintaining homeostasis in the central nervous system such as the provision of metabolic support, buffering of ions, recycling

neurotransmitters and formation of the blood brain barrier [3]. Astrocytes are also known to influence oligodendrocyte development by modulating the availability of growth factors and nutrients required for oligodendrocyte differentiation [4]. Astrocyte activation in response to CNS injury can have both protective and detrimental effects on overall neuronal survival and myelination [5]. In this study, we aimed to study the effect of hypoxia on astrocytes to delineate the pathways that could potentially impact oligodendrocyte maturation.

Transcriptomic analysis of human fetal neural stem cell-derived astrocytes subjected to hypoxia demonstrated the upregulation of cholesterol biosynthetic pathways. These findings were validated by measuring the gene and protein expression of cholesterol synthetic and transport proteins in FNSC-derived astrocytes and in a cell line model. Astrocyte cholesterol content and efflux was also increased in response to hypoxia. However, premyelinating oligodendrocytes did not

* Corresponding author at: Department of Biochemistry, All India Institute of Medical Sciences, Ansari Nagar 3027A, New Delhi 110029, India.

E-mail address: sudipsen665@gmail.com (S. Sen).

Abbreviations

ABCA1	ATP-binding cassette transporter 1
ApoE	apolipoprotein E
BSA	bovine serum albumin
CA9	carbonic anhydrase IX
DMEM	Dulbecco's modified Eagle's medium
EAAT	excitatory amino acid transporter
FBS	fetal bovine serum
FNSC	fetal neural stem cell
GFAP	glial fibrillary acidic protein
HIF1 α	hypoxia inducible factor 1 α
HMGCR	hydroxy-methyl-glutaryl-coenzyme A reductase
LDLR	low density lipoprotein receptor
MBP	myelin basic protein
NES	normalised enrichment score
OPC	oligodendrocyte progenitor cells
PMA	phorbol myristate acetate
SQLE	squalene epoxidase
SRB1 (SCARB1)	scavenger receptor B1

upregulate cholesterol synthesis in response to hypoxia. Coculture studies established that oligodendrocytes demonstrated increased levels of astrocyte derived cholesterol after hypoxic injury as compared to normoxic controls and supplementation of cholesterol increased oligodendroglial maturation.

Our findings therefore underline the differences in glial cholesterol production and distribution in hypoxic injury in an *in vitro* model and suggest that increased astrocyte cholesterol synthesis could supplement oligodendroglial maturation and serve as a neuroprotective mechanism in these pathological conditions.

2. Methodology

2.1. Ethics approval

Appropriate clearances were obtained from Institute ethics committee (Approval number: IEC-180/07.04.2017, RP-27/2017) and Institutional Committee for Stem Cell Research (Approval number:IC-SCR/66/17(o)), All India Institute for Medical Sciences, New Delhi prior to start of the study.

2.2. Cell culture

Astrocytes were differentiated from human fetal neural stem cells as previously described [6]. Briefly, human fetal neural stem cells were isolated from the brains of aborted human fetuses and differentiated into astrocytes over a period of 14 days using Dulbecco's Modified Eagle's Medium with high glucose [Catalog# AL007A, Himedia, Mumbai, MH, INDIA] containing 10 % fetal bovine serum [Catalog# 10270–106 GIBCO, NY, USA] and penicillin (50 IU/mL) and streptomycin (50 μ g/mL) [Catalog#15070–063, GIBCO, NY, USA]. Half the media was changed every alternate day and cells were harvested for experiments using 0.25 % Trypsin with EDTA [Catalog# 25200056, GIBCO, NY, USA]. Cells were characterised by the expression of astrocyte specific glial fibrillary acidic protein (GFAP) and excitatory amino acid transporters (EAAT1 and EAAT2).

SVG cell line resembling astrocytes (gifted by Dr. Pankaj Seth, NBRC) and Mo3.13 cells (obtained from Cedar Lane, Ontario, Canada [Catalog# CLU301]) resembling premyelinating oligodendrocytes, were maintained in DMEM-high glucose with 10 % FBS and penicillin-streptomycin. Media was changed every alternate day and cells were harvested for experiments using 0.25 % Trypsin with EDTA. For

differentiation of Mo3.13 into mature myelin producing oligodendrocytes, media was changed to DMEM-high glucose with FBS with either 100 nM phorbol-myristate acetate (PMA)[Sigma Aldrich, MO, USA Catalog#P1585] alone or in combination with 16 μ M cholesterol [Himedia, Mumbai, MH, INDIA Catalog#57–88-5] or 0.2 % ethanol (vehicle control)[Catalog#100983, Merck, Darmstadt, Germany].

For hypoxia experiments cells were exposed to 0.2 % oxygen, 5 % carbon dioxide and 94.8 % nitrogen or 20 % oxygen, 5 % carbon dioxide and 75 % nitrogen at 37 °C in a Baker Ruskin [Bridgend, UK] hypoxia unit [PhO2x box] for 48 hours.

2.3. Cocultures and colocalization analysis

SVG cells were harvested, washed and counted before staining by incubation for 1 h in labelling media containing DMEM-high glucose, 0.2 % bovine serum albumin (Sigma, MO, USA Catalog #A9418), 2.5 μ M BODIPY cholesterol [Sigma, MO, USA 810255P], unlabelled cholesterol (molar ratio of 1:4 labelled:unlabelled cholesterol) and methylcyclodextrin [Sigma, MO, USA Catalog#C4555] (molar ratio 1: 40 cholesterol:cyclodextrin). Labelling media was filtered with 0.45 μ m filter prior to use. Mo3.13 cells were harvested, washed and counted before staining with CellBrite Biotium Red Membrane Dye [Biotium, CA, USA Catalog# 30023] according to the manufacturer's protocol. Labelled cells were washed thoroughly with phosphate buffered saline and 1×10^5 cells of each type were plated together onto 6 well plates for further experiments.

Cocultures were visualised under a laser scanning confocal microscope [Nikon Ti-E 601869] and images obtained were analysed using JaCOP plugin on ImageJ to calculate the Pearson's correlation coefficient.

2.4. RNA isolation, cDNA synthesis and qPCR

Total RNA was isolated from cells using Trizol [Sigma, MO, USA Catalog#TR118] according to the manufacturer's protocol and quantified using a NanoDrop [ND1000, Thermo-Fisher Scientific, MA, USA]. cDNA was synthesised using M-MuLV RT [Thermo-Fisher Scientific, MA, USA Catalog# EP0442] and random hexamer primers (Thermo-Fisher Scientific, MA, USA Catalog #30142). For evaluating gene expression, qPCR was carried out using gene specific primers (Table 1) and DyNAamo Flash SYBR Green qPCR kit [Thermo-Fisher Scientific, MA, USA Catalog #F416L] using a qPCR system [G8830A, Agilent, Santa Clara, CA, USA]. Ct value obtained was normalised using 18S rRNA as a reference gene. Fold changes were calculated using the $2^{-\Delta\Delta CT}$ method using appropriate controls.

2.5. RNA sequencing and transcriptomic analysis

RNA concentration and integrity were analysed using Nanodrop (One^C, Thermo Fisher Scientific, MA, USA) and Bioanalyzer (Agilent, Santa Clara, CA, USA), respectively. A modified NEB Next RNA Ultra protocol was used to prepare the libraries for total RNA sequencing. Whole transcriptome sequencing was performed using Illumina HiSeq 4000 system to generate 60 million reads, 2 × 100 bp reads/sample. Sequenced data was processed to generate FASTQ files. The quality of

Table 1
Sequences of primers used for gene expression analysis.

Gene	Forward primer	Reverse primer
18S rRNA	GTAACCGTGTGAACCCCATT	CCATCCAATCGTAGTAGCG
HMGCR	TAGTGAGATCTGGAGGATCAA	CTGTCCCCACTATGACTTCCC
SQLE	GGTGCCTCTCTACCGCTGTGTC	GGTTCCCTTTCTGCCCTCC
ABCA1	AATCCTGACCGGGTTGTTC	TCTGATTCCACCTGACAGC
APOE	TGGAGCAAGCGGTGGAGACAG	TCTCGTCCATCAGGCCCTC
LDLR	CAAGCTCTGGCGACGTT	AAAGGAAGACGAGGAGCACGAT
SCARB1	CTTCCAGGATGTCCCT	ATGCCAGAAGTCACCTTG

these reads were checked by FastQC. The paired-end reads are aligned to the reference human genome (hg19). Alignment was performed using HISAT2 (2.1.0). The aligned reads were used for estimating the expression of the genes. The raw read counts were estimated using FeatureCount (1.5.2). Read count data were normalised using DESeq2. Gene set enrichment analysis (GSEA) for various gene ontology terms and pathways was done using iDEP 0.91:an integrated web application for differential expression and pathway analysis of RNA-Seq data.

2.6. Protein isolation, quantification and Western blotting

Cells were lysed in RIPA lysis buffer with protease inhibitors, and the protein concentration in lysates was determined using the bicinchoninic acid assay (BCA) (Pierce, Thermo Fisher Scientific, MA, USA Catalog# 23227). 40 µg lysate was loaded into each well for SDS-PAGE (4 % stacking gel, 8–12 % resolving gel). Proteins were blotted onto a 0.22-µm nitrocellulose membrane, followed by blocking in 5 % non-fat milk (NFM) in TBS. Blots were incubated overnight at 4 °C with primary antibody (Table 2) diluted in 1 % NFM, followed by three washes with TBST. Blots were then incubated for 1 h with the corresponding secondary antibody diluted in 1 % NFM. This was followed by four washes in TBST. The blot was incubated with Luminol and peroxidase (Abbkine SuperLumia ECL Plus Kit, Hubei, China), and chemiluminescence detection was performed using an Azure Biosystems C280 gel documentation system (Dublin, CA, USA), followed by analysis with ImageJ software. Normalization was performed using β-actin protein level.

2.7. Flow cytometry

Cells were fixed with 2 % paraformaldehyde and permeabilized with 1 % BSA containing 0.1 % Triton X-100. Cells were blocked with 2 % BSA for half an hour and subsequently stained with appropriate primary antibody. Cells were washed and then incubated with the secondary antibody (Table 2) for 1 h in the dark. Cells were washed and resuspended in 2 % paraformaldehyde, and data were acquired using BD LSR Fortessa (BD Biosciences, San Jose, CA, USA) and analysed using FlowJo v10 software.

2.8. Cholesterol estimation by AmplexRed assay

Cells were lysed in methanol followed by extraction of lipids using phase separation in methyl tert-butyl ether (MTBE) and phosphate buffered saline (PBS). Organic phase containing cellular lipids was dried under nitrogen and dried lipid was resuspended in assay buffer prior to analysis. Total cholesterol in cell culture supernatants and cells was measured using AmplexRed Cholesterol assay [ThermoFisher Scientific, MA, USA Catalog# A12216] as per the manufacturer's protocol.

2.9. Statistical analysis

All experiments were performed in at least 3 independent experiments. Statistical analysis was performed using GraphPad Prism v9. Statistical differences were analysed using Mann-Whitney or Wilcoxon matched signed rank test (for two groups) or two-way ANOVA followed by Tukey's test (>2 groups). *p*-values <0.05 were considered significant.

3. Results

3.1. Transcriptomic analysis of human fetal neural stem cell-derived astrocytes after exposure to hypoxia

Human fetal neural stem cells were isolated and differentiated into astrocytes as described previously [6]. Differentiated astrocytes were exposed to hypoxia (0.2 % oxygen) for 48 h which was confirmed by increased expression of HIF1α on Western blot (Fig. 1a). After appropriate quality control, total cellular RNA was sequenced (*n* = 3 samples

Table 2

Specifications for primary and secondary antibodies used in western blot and flow cytometry experiments.

Antibody	Molecular weight (kDa)	Antibody specifications	Used In	Procured from
Anti-MBP (2H9) (Catalog # NBP2-22121)	33, 18	Monoclonal Mouse IgG1	Flow Cytometry (3 µl/ million cells)	Novus Biologicals, CO, USA
Anti-HIF1α (Catalog # #36169S)	120	Monoclonal Rabbit IgG	Western blotting (1:1000)	CST, Danvers, MA, USA
Anti-β-actin (Catalog # STJ94020)	42	Polyclonal Rabbit IgG	Western Blotting (1:2000)	St. John's Laboratory, UK
Anti-HMGCR (Catalog # #A1633)	97	Polyclonal Rabbit IgG	Western Blotting (1:1000)	Abclonal, MA, USA
Anti-SQLE (Catalog # A2428)	65	Polyclonal Rabbit IgG	Western Blotting (1:2000)	Abclonal, MA, USA
Anti-ABCA1 (Catalog # 7228)	245	Polyclonal Rabbit IgG	Western blotting (1:1000)	Abclonal, MA, USA
Anti-APOE (Catalog # 16344)	34	Polyclonal Rabbit IgG	Western blotting (1:500)	Abclonal, MA, USA
Alexa Fluor™ 647 Anti-GFAP (Catalog # 561470)	—	Monoclonal Mouse IgG2b	Flow Cytometry (3 µl/ million cells)	BD, Biosciences, CA, USA
Alexa Fluor™ 488 Rabbit anti-mouse IgG, (Catalog # A110059)	—	Rabbit anti-Mouse IgG (H + L) Cross-Adsorbed	Flow Cytometry (1:200)	Thermo Fisher Scientific, MA, USA
Alexa Fluor™ 488 Goat anti-Mouse IgG, (Catalog # A-11004)	—	Secondary Antibody, Alexa Fluor™ 488	Flow cytometry (1:200)	Thermo Fisher Scientific, MA, USA
Alexa Fluor™ 594 Goat anti-Mouse IgG, (Catalog # A-11008)	—	Secondary Antibody, Alexa Fluor™ 568	Flow cytometry (1:200)	Thermo Fisher Scientific, MA, USA
HRP-tagged Anti-rabbit secondary antibody (Catalog # 7074S)	—	Goat Anti-Rabbit IgG (H + L) Cross-Adsorbed	Western Blotting (1:2000)	Invitrogen™, Fisher Scientific

each for normoxia and hypoxia). 1365 genes were found to be differentially expressed (log2fold change>1 and adjusted *p*-value<0.1) out of which 585 were upregulated while 780 were downregulated in astrocytes exposed to hypoxia as compared to normoxic controls (Fig. 1b, Supplementary Table S1 and S2). Gene set enrichment analysis to look for key gene ontology terms affected in hypoxic injury to astrocytes (Supplementary Table S3 and S4) revealed that terms relating to sterol and cholesterol biosynthetic pathways (normalised enrichment score (NES) 2.35, adjusted *p*-value 0.004) were positively enriched in hypoxic astrocytes (Fig. 1c). Pathway analysis (Supplementary table S5 and S6) showed the positive enrichment of HIF 1 signaling pathway (NES 2.06, adjusted *p*-value 0.0034) validating the hypoxia exposure in our *in vitro* model. Moreover, steroid biosynthesis (NES 2.42, adjusted *p*-value 0.0029) and terpenoid backbone synthesis (NES 1.93, adjusted *p* value

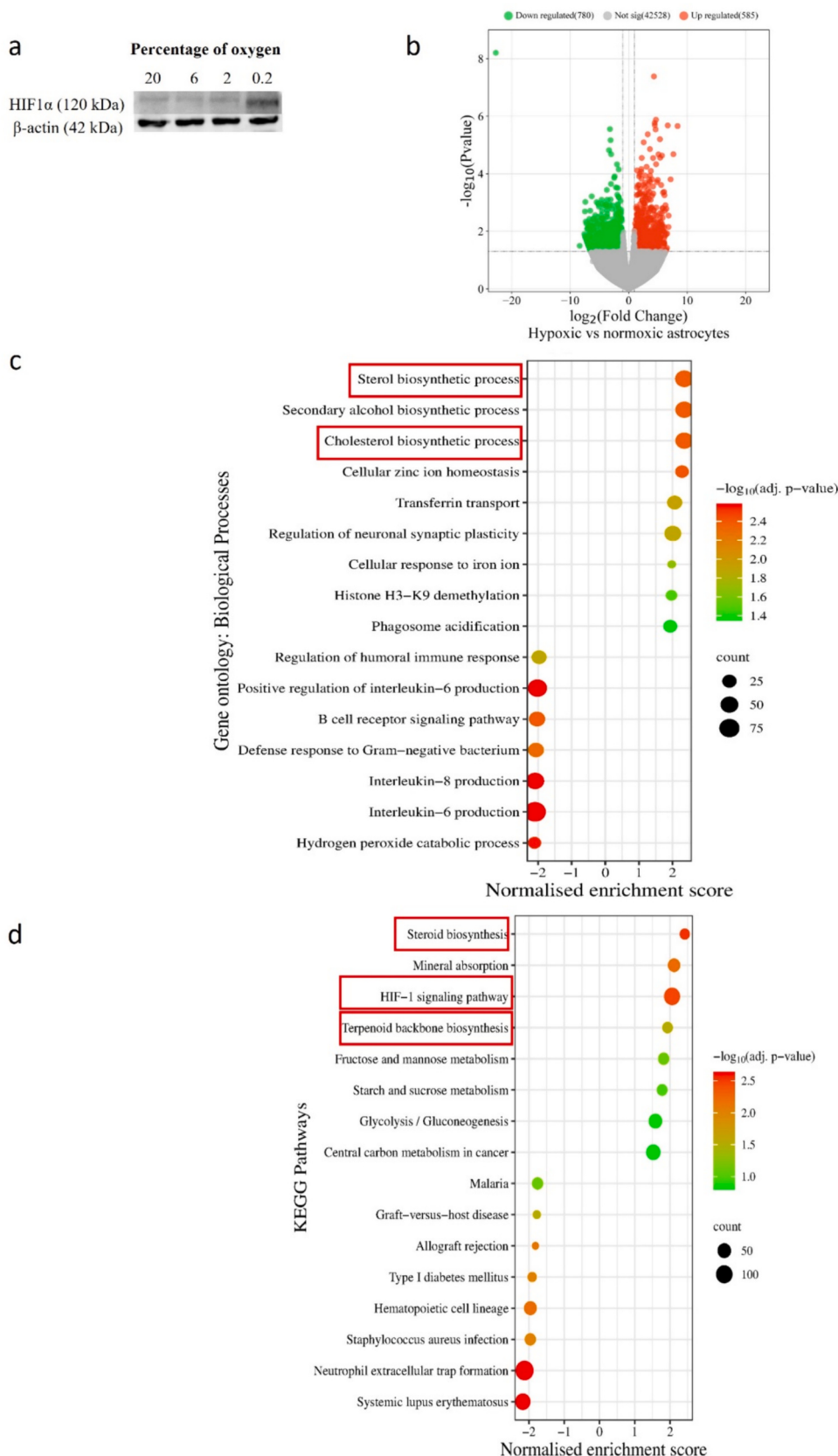


Fig. 1. Transcriptomic analysis of hypoxia exposed FNSC derived-astrocytes. **a:** Representative western blot of HIF1 α expression in astrocytes exposed to different concentrations of oxygen (β -actin is used as loading control). **b:** Differentially expressed genes in astrocytes exposed to 0.2 % oxygen (hypoxia) as compared to those exposed to 20 % oxygen (normoxia). Gene set enrichment analysis of gene ontology terms (**c**) and pathways (**d**) differentially enriched in hypoxic astrocytes.

0.03) pathways were positively enriched in astrocytes exposed to hypoxia (Fig. 1d). Pathway mapping showed that the gene expression of most of the enzymes involved in terpenoid backbone synthesis and steroid biosynthesis was increased on exposure to hypoxia (Fig. 2a).

Cholesterol synthesis increases after hypoxia in FNSC-derived astrocytes as well as in a cell line model.

On the basis of the above results, further validation was carried out to assess cholesterol synthesis and transport in FNSC-derived astrocytes exposed to hypoxia. Hypoxia-exposed astrocytes showed an upregulation of cholesterol synthetic genes hydroxy-methyl-glutaryl CoA reductase (HMGCR; fold change 3.9 ± 0.83 , $p = 0.02$) and squalene epoxidase (SQLE; fold change 4 ± 2.4 , $p = 0.008$) on qPCR (Fig. 2b and c). There was also an upregulation of cholesterol efflux protein ABCA1 (fold change 2.4 ± 0.5 , $p = 0.03$) and transport apolipoprotein ApoE (fold change 1.29 ± 0.16 , $p = 0.027$) on qPCR (Fig. 2d, e). Protein expression of HMGCR (normalised expression 0.7 ± 0.17 in normoxia and 1.13 ± 0.14 in hypoxia, $p = 0.015$), SQLE (normalised expression 0.4 ± 0.08 in normoxia and 1.1 ± 0.27 in hypoxia, $p = 0.031$), ABCA1 (normalised expression 0.9 ± 0.18 in normoxia and 1.1 ± 0.3 in hypoxia, $p = 0.6$) and ApoE (normalised expression 0.3 ± 0.004 in normoxia and 0.5 ± 0.1 in hypoxia, $p = 0.125$) was also measured by western blot and was found to be increased after hypoxia (Fig. 2 f-j).

These findings were further duplicated in a cell line model of human astrocytes *viz.* SVG. This cell line has been used extensively to model astrocytes *in vitro* [7,8]. On flow cytometric analysis, approximately 96 % SVG cells expressed astrocyte-specific marker GFAP (Fig. 3a,b) and did not express oligodendrocyte marker protein MBP (Fig. 3c,d). SVG cells exposed to hypoxia also demonstrated an increase in HIF1 α downstream molecule CA9 (Fig. 3e: fold change 184.4 ± 63.3 $p = 0.0075$). There was increased expression of SQLE (fold change 1.9 ± 0.3 , $p = 0.0079$), APOE (fold change 1.6 ± 0.3 , $p = 0.021$) and ABCA1 (fold change 1.6 ± 0.3 , $p = 0.008$) on qPCR (Fig. 3 g-i) while there was a decrease in gene expression of HMGCR (Fig. 3f: fold change 0.8 ± 0.6 , $p = 0.13$), which was not found to be significant. Western blot analysis confirmed the increased expression of the proteins HMGCR (normalised expression 1.02 ± 0.31 in normoxia and 1.5 ± 0.56 in hypoxia, $p = 0.031$) and SQLE (normalised expression 0.67 ± 0.34 in normoxia and 1.4 ± 0.66 in hypoxia, $p = 0.003$) in astrocytic cells after exposure to hypoxia. Expression of HIF1 α (normalised expression 0.27 ± 0.15 in normoxia and 0.5 ± 0.3 in hypoxia, $p = 0.125$) and ABCA1 (normalised expression 1.06 ± 0.3 in normoxia and 1.2 ± 0.3 in hypoxia, $p = 0.15$) was also increased on exposure to hypoxia, however, significance was not attained ($p > 0.05$ for both) (Fig. 3j-n).

Cholesterol was measured intracellularly (Fig. 3o: 13.7 ± 2.9 $\mu\text{g}/\text{mg}$ protein in normoxia and 27 ± 8.2 $\mu\text{g}/\text{mg}$ protein in hypoxia, $p = 0.057$) and in the supernatant (Fig. 3p: 2 ± 0.5 $\mu\text{g}/\text{mg}$ protein in normoxia and 2.8 ± 0.3 $\mu\text{g}/\text{mg}$ protein in hypoxia, $p = 0.025$) of SVG cells exposed to hypoxia using a fluorometric enzyme-based assay and was found to be increased, indicating an increase in the synthesis and efflux of cholesterol by these cells under hypoxic conditions. Flow cytometric analysis showed that hypoxia exposure resulted in an increase in the cell surface expression of ABCA1 (Fig. 3q) which facilitates ApoE mediated efflux of cholesterol from cells (Median fluorescence intensity $11,053 \pm 275$ in normoxia and 1819 ± 177.8 in hypoxia, $p = 0.028$).

3.2. Oligodendrocyte cells do not upregulate cholesterol synthesis in response to hypoxia

As premyelinating oligodendrocytes are more vulnerable to hypoxic injury, the effect of hypoxia on cholesterol synthesis in this cell type was studied using a cell line model Mo3.13 resembling premyelinating oligodendrocytes. The Mo3.13 cells were treated with PMA to differentiate them into mature myelinating oligodendrocytes. On exposure to hypoxia, Mo3.13 cells showed an upregulation of the hypoxia-responsive gene CA9 (Fig. 4a: fold change 93.31 ± 78.9 , $p = 0.001$) while the expression of cholesterol synthetic genes HMGCR (fold change $0.8 \pm$

0.14 , $p = 0.0079$) and SQLE (fold change 0.6 ± 0.4 , $p = 0.0074$) was decreased on qPCR (Fig. 4b, c). Though these changes were mirrored in the decreased protein expression of HMGCR (Normalised expression 0.31 ± 0.2 in normoxia and 0.25 ± 0.1 in hypoxia) and SQLE (normalised expression 0.6 ± 0.4 in normoxia and 0.3 ± 0.2 in hypoxia) after hypoxia on Western blot analysis (Fig. 4 f-i), there was an expected increase in the HIF1 α protein expression (normalised expression 0.15 ± 0.06 in normoxia and 1.3 ± 0.16 in hypoxia, $p = 0.025$). Interestingly the expression of the LDL-receptor (LDLR) was increased in premyelinating oligodendrocytes exposed to hypoxia (Fig. 4d: fold change 1.4 ± 0.2 , $p = 0.0005$) while expression of SRB1 was decreased (Fig. 4e: fold change 0.7 ± 0.2 , $p = 0.0075$). The cholesterol content of Mo3.13 cells was also decreased following hypoxia exposure (Fig. 4f: 30 ± 2.3 $\mu\text{g}/\text{mg}$ protein in normoxia 17 ± 6.4 $\mu\text{g}/\text{mg}$ protein in hypoxia).

Cholesterol is an essential component of myelin and steroid biosynthesis is one of the pathways upregulated in oligodendrocytes during their differentiation [9]. Mo3.13 cells can be differentiated into cells resembling mature oligodendrocytes on treatment with PMA. We also found that there was increased expression of cholesterol synthetic proteins HMGCR (normalised expression 0.8 ± 0.3 , $p = 0.04$) and SQLE (normalised expression 1.12 ± 0.7) on differentiation of Mo3.13 cells using PMA. Although differentiated cells also showed a decrease in the protein expression of HMGCR (normalised expression 0.6 ± 0.08) the expression of SQLE (normalised expression 1.1 ± 0.7) on hypoxia exposure remained unchanged, indicating that oligodendrocyte populations at different developmental stages showed differences in cholesterol synthetic response in conditions of hypoxic injury (Fig. 4f-i).

3.3. Cholesterol transfer between astrocytes and oligodendrocytes is increased in response to hypoxia

To assess the effect of hypoxia exposure on the transfer of cholesterol from astrocytes to oligodendrocytes, cocultures of SVG and Mo3.13 cells were established. SVG cells were labelled with fluorescent BODIPY cholesterol while Mo3.13 cells were labelled with a red membrane dye (Fig. 5a). Cholesterol transfer was estimated by measuring the fluorescent-cholesterol in labelled Mo3.13 cells by flow cytometry and confocal imaging. After 48 h of coculture there was an increase in the colocalization between cholesterol and red membrane label on confocal imaging (Fig. 5b: correlation coefficient 0.07 ± 0.009 at 12 h of coculture and 0.47 ± 0.04 at 48 h of coculture, $p = 0.029$), indicating transport of cholesterol from SVG to Mo3.13 cells. On exposure of the cocultures to hypoxia there was an increase in the percentage of Mo3.13 cells with fluorescent cholesterol (percentage of double positive cells after 48-h cocultures was 8.5 ± 1 in normoxia and 20.5 ± 1.9 in hypoxia) as measured by flow cytometry, signifying increased SVG-derived cholesterol content in these cells after hypoxia (Fig. 5 c-f).

3.4. Cholesterol promotes differentiation of pre-myelinating oligodendrocytes to mature oligodendrocytes

Mo3.13 cells were differentiated in the presence of PMA or PMA with cholesterol along with a vehicle control. Cells differentiated in the presence of cholesterol showed increased expression of MBP after differentiation as measured by flow cytometry. The percentage of MBP positive cells (Fig. 5g) increased significantly from 11.05 ± 1.4 in undifferentiated cells to $33.0.8 \pm 8.6$ in cells differentiated with PMA alone ($p = 0.06$), 39.2 ± 13.6 in cells differentiated using PMA with ethanol (vehicle control; $p = 0.0071$) and 61.2 ± 6.2 in cells differentiated using PMA in combination with cholesterol ($p < 0.0001$). Significant increase in percentage of MBP positive cells was found in cells differentiated in PMA with cholesterol as compared to PMA alone ($p = 0.023$). Median fluorescence intensity of MBP expression on flow cytometric analysis (Fig. 5h) also increased on differentiation (224.8 ± 22.6 in undifferentiated, 386 ± 152.6 in PMA differentiated, 357.8 ± 17.8 in vehicle and 694.5 ± 208.5 in PMA + cholesterol). However, significant increase was

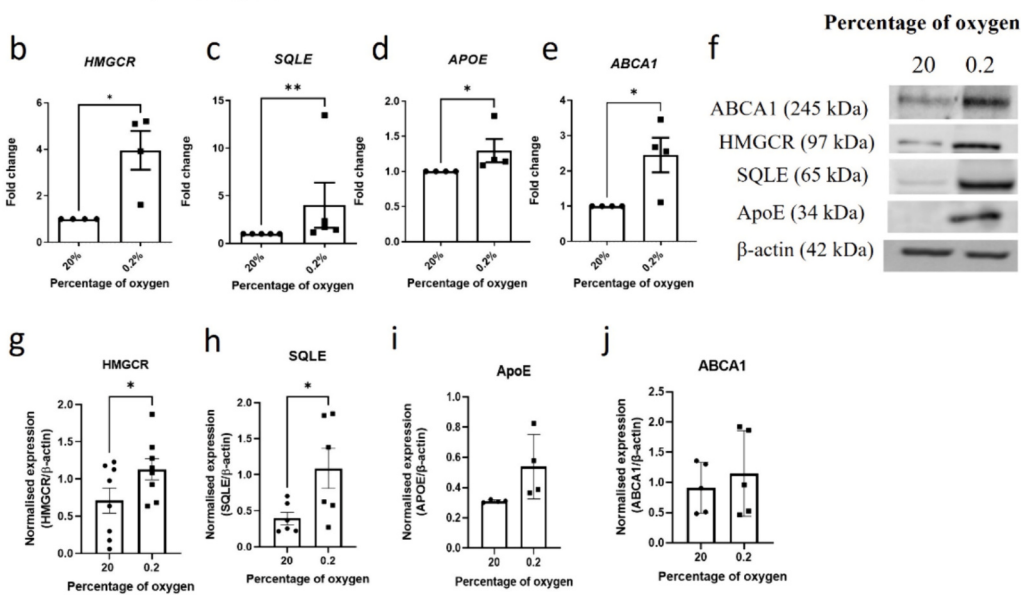
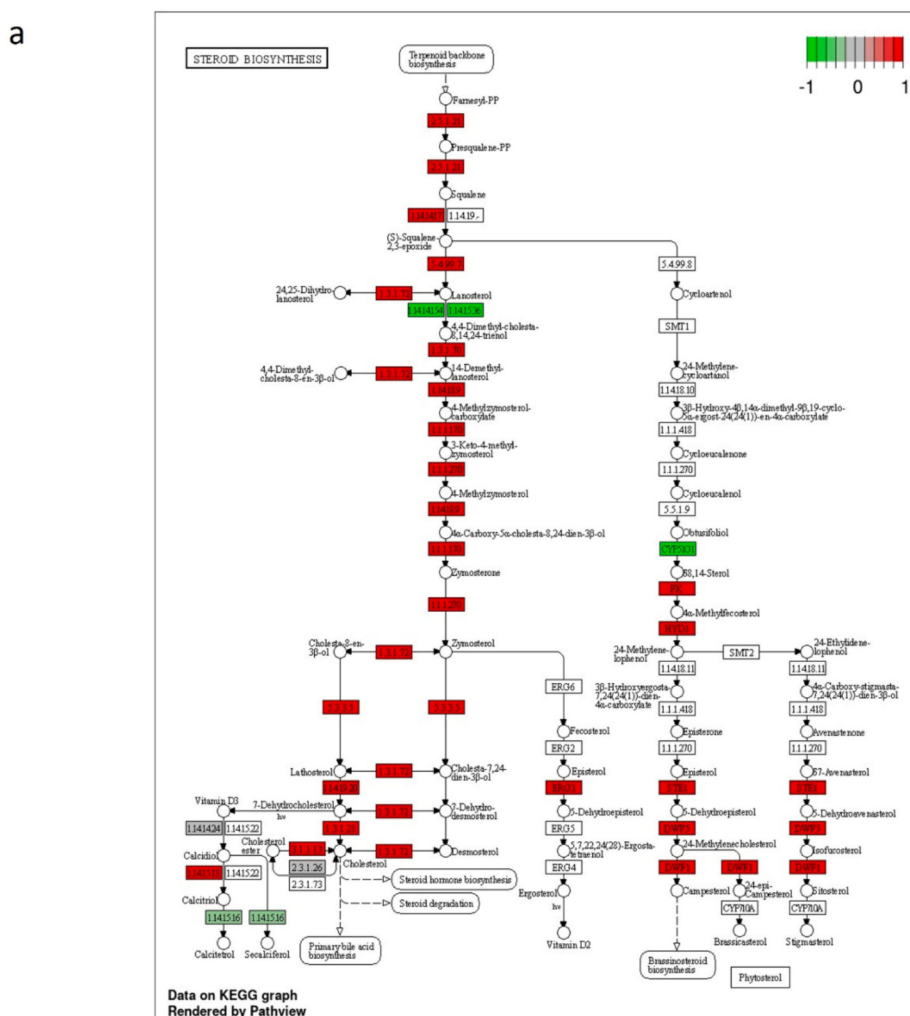


Fig. 2. Expression of cholesterol synthetic and transport proteins in hypoxia-exposed FNSC-derived astrocytes. a. Pathway map of differentially expressed genes in cholesterol synthetic pathway in hypoxia exposed astrocytes (generated using iDEP 0.96 KEGG Pathview pathway analysis). Gene expression of HMGCR (b), SQLE (c), APOE (d) and ABCA1(e) in hypoxia exposed astrocytes and normoxic controls as analysed by qPCR ($n = 4-5$). Representative western blots (f) and densitometric quantification of protein expression of HMGCR(g), SQLE (h), APOE(i) and ABCA1(j) in hypoxia exposed astrocytes along with normoxic controls ($n = 4-7$). Data represented as Mean \pm SEM. * $p < 0.05$, ** $p < 0.01$.

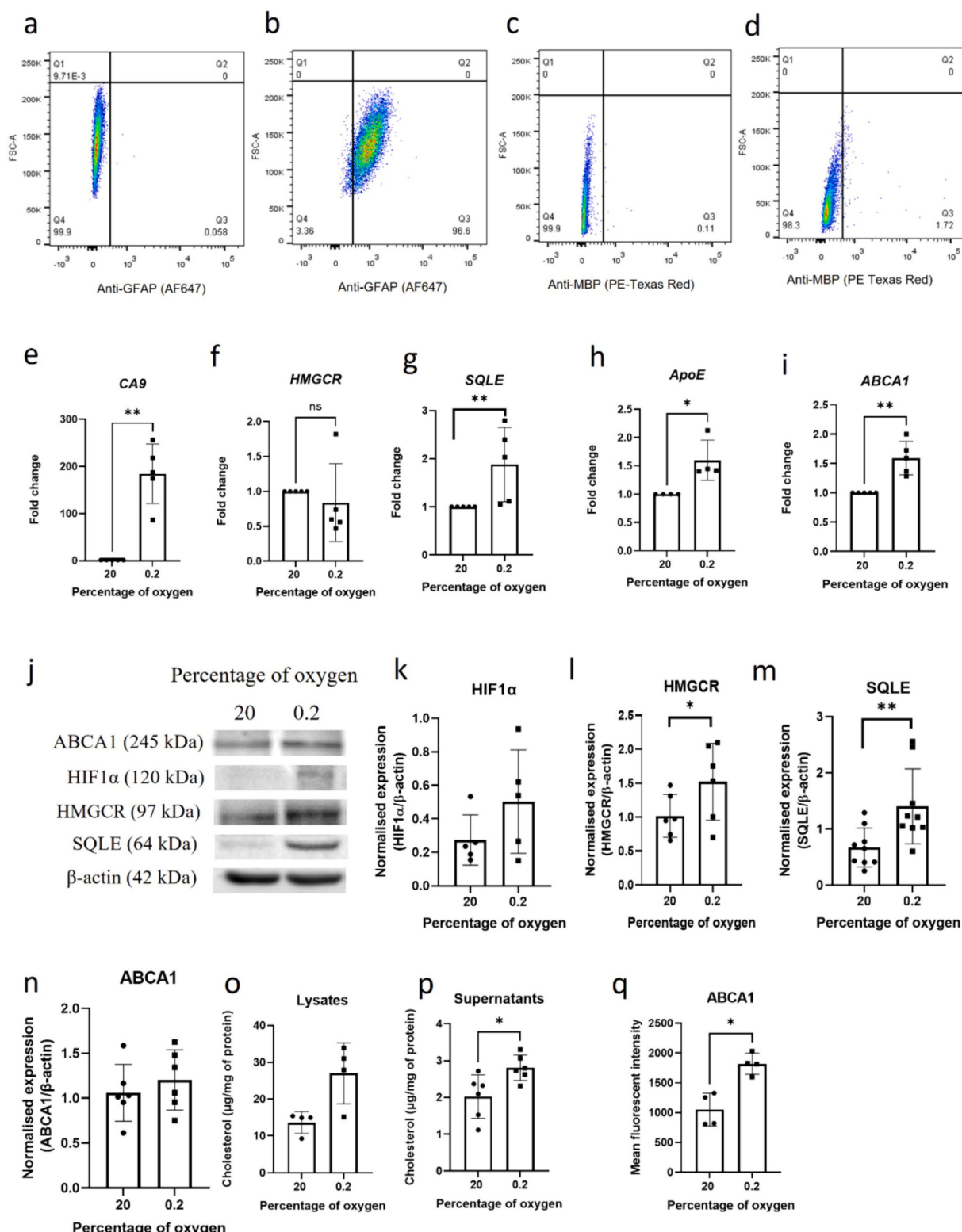


Fig. 3. Expression of cholesterol synthetic and transport proteins in astrocytic cell line (SVG) exposed to hypoxia. Representative dot-plots of SVG cells evaluated for the expression of GFAP (a: unstained, b: stained with anti-GFAP antibody) and MBP (c: unstained, d: stained with anti-MBP antibody) by flow cytometry. Gene expression of CA9 (e), HMGCR (f), SQLE (g), APOE (h) and ABCA1(i) in hypoxia exposed SVG and normoxic controls as analysed by qPCR ($n = 4-5$). Representative western blots (j) and densitometric quantification of protein expression of HIF1 α (k), HMGCR(l), SQLE (m), and ABCA1(n) in hypoxia exposed SVG along with normoxic controls ($n = 5-8$). Quantification of total cholesterol in cell lysates (o) and supernatants (p) of hypoxic and normoxic SVG cells ($n = 6$). (q) Quantification of ABCA1 surface expression in hypoxic and normoxic astrocytes as measured by flow cytometry ($n = 4$). Data represented as Mean \pm SD. * $p < 0.05$, ** $p < 0.01$.

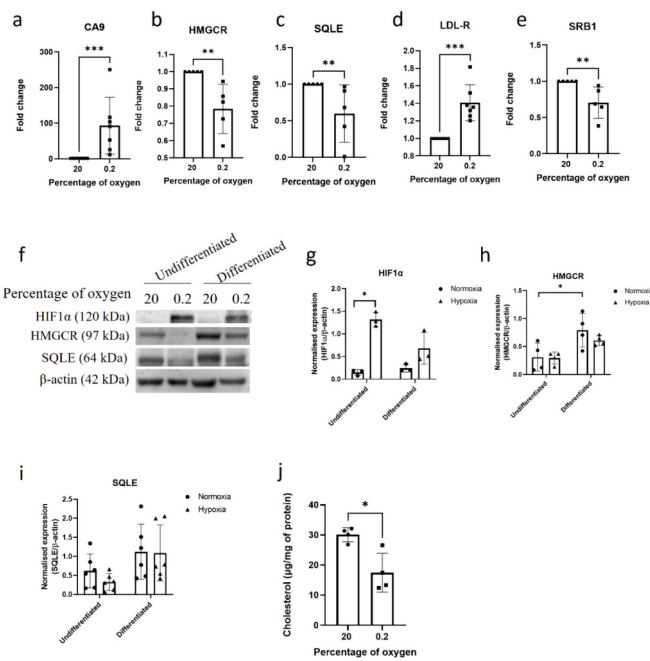


Fig. 4. Expression of cholesterol synthetic and transport proteins in oligodendrocytes exposed to hypoxia. Gene expression of CA9 (a), HMGCR (b), SQLE (c), LDL-R (d) and SRB1(e) in hypoxia exposed premyelinating oligodendrocyte cell line (Mo3.13) as analysed by qPCR ($n = 5-6$). Representative western blots (f) and densitometric quantification of protein expression of HIF1 α (g), HMGCR(h) and SQLE (i) in hypoxia exposed premyelinating (undifferentiated) and matured (differentiated) oligodendrocytes along with normoxic controls ($n = 3-6$). Quantification of total cholesterol in cell lysates (j) of hypoxia exposed premyelinating oligodendrocytes ($n = 3$). Data represented as Mean \pm SD. * $p < 0.05$, ** $p < 0.01$ *** $p < 0.001$.

only seen in cells differentiated using PMA with cholesterol ($p = 0.001$).

4. Discussion

Hypoxic injury to the preterm brain leads to death of vulnerable premyelinating oligodendrocytes which are the most abundant oligodendroglial lineage cells in the brain at 27–32 weeks of gestation [10]. Hypoxic injury to premyelinating oligodendrocytes leads to failure of maturation and myelination [11]. Astrocytes influence oligodendroglial development through the secretion of growth factors and providing metabolic support in both physiological and pathological states [12]. In this study, the mechanisms by which altered astrocyte function in hypoxic conditions could impact oligodendrocyte development were investigated. A model of primary human astrocytes differentiated from fetal neural stem cells and characterised for the expression of astrocyte-specific proteins [6] was used. These hFNSC-derived astrocytes were exposed to hypoxia for 48 h which was validated by an increase in the expression of the hypoxia-responsive protein, HIF1 α . Transcriptomic changes in hypoxia-exposed astrocytes interestingly revealed upregulation of pathways involved in steroid biosynthesis. The upregulated genes included key enzymes of the cholesterol biosynthetic pathway including HMG-CoA reductase (HMGCR), mevalonate kinase (MK) and squalene epoxidase (SQLE).

Cholesterol within the central nervous system is produced *de novo*, as cholesterol from the circulation cannot cross the blood-brain barrier. Within the CNS, cholesterol is produced by astrocytes, neurons as well as oligodendrocytes with astrocytes serving as a source for cholesterol for other cell types during times of need [13]. Cholesterol is transported in the form of ApoE-containing lipoproteins. Astrocytes express ABCA1 for the efflux of cholesterol and form lipoprotein-like particles which are taken up by oligodendrocytes and neurons using LDL-receptor (LDLR),

scavenger receptor class B type 1 (SRB1) or LDL-R related protein 1/2 (LRP1/2) [14]. In our study, we found that hypoxia increased the gene as well as protein expression of HMG-CoA reductase (HMGCR) and squalene epoxidase (SQLE) both in hFNSC-derived astrocytes and in a cell line model. Hypoxic astrocytes also showed the increased expression of apolipoprotein E (ApoE) and the cholesterol efflux protein (ABCA1). In the cell line model, hypoxia increased surface expression of ABCA1, indicating that astrocytes could potentially increase the efflux of cholesterol in such conditions. Indeed, when cholesterol was measured in astrocytes and their culture supernatants, there was increase in the cholesterol content in supernatants of hypoxia-exposed astrocytes compared to normoxic controls, highlighting that astrocytes not only produced more cholesterol in hypoxia, but also effluxed it into the surrounding medium. Our findings are in agreement with those of Smolic et al. [15] who found that astrocytes accumulate lipid droplets in conditions of stress.

The oligodendroglial responses to hypoxic injury was investigated using the Mo3.13 cell line. This cell line resembles premyelinating oligodendrocytes as has been previously validated earlier [9] and has been extensively used to model oligodendrocyte development [16,17]. Mo3.13 cells express cell type-specific markers of premyelinating oligodendrocytes (O4 and NG2) and can be differentiated into myelin basic protein (MBP)-expressing mature myelinating oligodendrocytes using phorbol-myristate-acetate (PMA). When undifferentiated Mo3.13 cells (resembling premyelinating oligodendrocytes) were exposed to hypoxia in our study, a downregulation of the expression of HMGCR and SQLE was observed, in contrast to astrocytes. Differentiation into mature oligodendrocytes induced an increase in the expression of these proteins, however, hypoxia exposure to differentiated oligodendrocytes did not result in decreased expression of SQLE, potentially indicating the differential response of oligodendrocyte developmental stages to hypoxic injury. Also, undifferentiated oligodendrocytes showed a decrease in their cellular cholesterol content on exposure to hypoxia. As oligodendroglial myelin forms a major part of the brain cholesterol pool, decrease in oligodendroglial cholesterol due to decreased synthesis (as reported here) or increased breakdown (as reported by [18]) could lead to overall reduction in brain cholesterol levels. Indeed, hypoxic injury was shown to decrease brain cholesterol and MBP levels in rats [19].

To investigate whether astrocyte cholesterol could be transferred to oligodendrocytes and the impact of hypoxia on this exchange, we generated coculture systems with fluorescent cholesterol-labelled astrocytes and membrane-labelled oligodendrocytes. Coculturing the two cell types under normal conditions demonstrated a transfer of the fluorescently labelled cholesterol from astrocytes to oligodendrocytes, as evidenced by the increased colocalization on flow cytometry as well as the presence of double positive cells on flow cytometry. Interestingly, after hypoxia exposure, the number of double-positive cells was increased in the cocultures, signifying more oligodendrocytes containing astrocyte-derived cholesterol in these conditions. Increased cholesterol synthesis and transfer by astrocytes can therefore supplement oligodendroglial cholesterol in hypoxic injury as oligodendrocytes themselves decrease cholesterol synthesis in these conditions. These findings support those of Camargo et al. [20] who found that disrupting oligodendroglial cholesterol synthesis resulted in only transient loss of myelination, whereas disruption of astrocytic cholesterol synthesis, resulted in sustained demyelination. Previous research has also shown that oligodendrocytes can take up astrocyte-derived cholesterol through lipoprotein-mediated mechanisms involving uptake through LDL-R, SRB1 or LRP1/2 receptors. Interestingly, we found that hypoxia exposure increased the gene expression of LDL-R but not SRB1 in premyelinating oligodendrocytes, suggesting that oligodendrocytes could take up cholesterol in hypoxic conditions through ApoE/LDL-R interactions as astroglial ApoE expression was also increased during hypoxia. Xie et al. [21] reported that disruption of oligodendroglial LDL-R causes demyelination in a mouse model of ischemic injury.

Lastly to test whether increased cholesterol delivery to

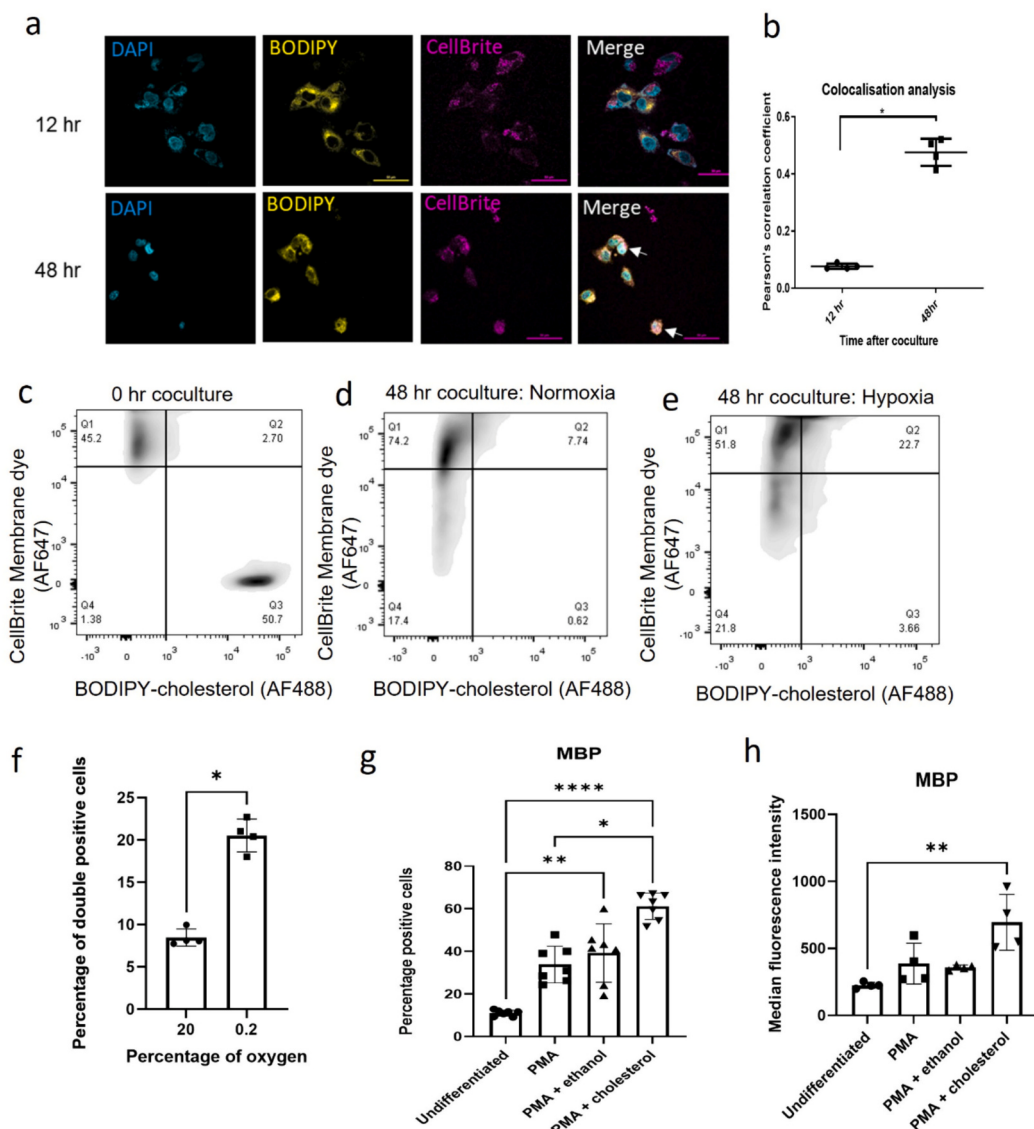


Fig. 5. Cholesterol transport in astrocyte-oligodendrocyte cocultures and effect of cholesterol treatment on oligodendrocyte maturation. **a.** Confocal microscopy of cocultures of BODIPY-labelled astrocytes (yellow) and CellBrite red membrane dye-labelled oligodendrocytes (magenta) at 12 h and 48 h of coculture. **b.** Quantification of colocalization of BODIPY-cholesterol and red membrane dye in astrocyte-oligodendrocyte cocultures at 12 h and 48 h after coculture ($n = 4$). Representative density plots of flow cytometric analysis of labelled astrocyte-oligodendrocyte cocultures at 0 h (c) and after 48 h of normoxia (d) and hypoxia (e). Quantification of cholesterol transport to oligodendrocytes as the number of double positive cells in cocultures (f) after 48 h of normoxia and hypoxia ($n = 4$). Evaluation of differentiation of premyelinating oligodendrocytes after treatment with PMA or PMA with alcohol (vehicle control) or PMA with cholesterol, by measuring the number of MBP positive cells (g) and median fluorescent intensity of MBP staining (h) after 3 days using flow cytometry ($n = 4-7$).

oligodendrocytes can influence oligodendrocyte maturation, we treated premyelinating oligodendrocytes with a standard differentiating agent (PMA) with or without exogenous cholesterol. Cholesterol-treated cells showed an increase in the expression of the mature oligodendrocyte marker MBP, signifying that supplemental cholesterol can increase the differentiation of premyelinating oligodendrocytes to mature oligodendrocytes. These findings are in agreement with previous studies which document the importance of cholesterol in oligodendrocyte differentiation and myelination [22,23].

Our novel findings therefore demonstrate that astrocytes increased cholesterol synthesis in hypoxic conditions, in contrast to premyelinating oligodendrocytes. The astrocytic cholesterol can be transferred to oligodendrocytes and this exchange is increased in conditions of hypoxic injury. Increased cholesterol delivery to premyelinating oligodendrocytes can result in increased maturation of these cells to myelinating oligodendrocytes. This is the first study that describes the expression of

cholesterol synthetic and transport proteins in glial cell populations in hypoxic injury and highlights the differences in cholesterol synthesis in glial populations in hypoxic injury. This is also one of the few studies implicating astrocyte-derived cholesterol supplementing oligodendroglial maturation in hypoxic injury and the first to demonstrate the glial cholesterol redistribution in hypoxic injury. As premyelinating oligodendrocytes are particularly susceptible to hypoxic injury, this could be an important mechanism by which astrocytes mediate neuroprotection in these conditions, adding to the already available evidence of astrocytes' neuroprotective role in these conditions.

Our study provides valuable insights into glial cholesterol redistribution in hypoxic injury; however a few caveats must be recognised. Our model investigates glial interactions *in vitro* which will need to be further validated in more complex systems *in vivo*. Inflammation resulting from neuronal cell death and demyelination is another factor that could affect the cholesterol dynamics and warrants further investigation. Also,

although we specifically outline cholesterol synthetic and transport pathways, other potential mechanisms also exist by which astrocytes might modify oligodendroglial maturation in hypoxic injury.

Arrest of oligodendrocyte maturation at the vulnerable premyelinating-oligodendrocyte stage is an important reason for the demyelination seen in hypoxic brain injury. The response of surrounding astrocytes to hypoxic injury can be relevant for disease pathogenesis as they are known to influence oligodendrocyte development. We discovered that astrocytes increase cholesterol synthesis after hypoxic injury, in contrast to premyelinating oligodendrocytes. Cholesterol efflux and transfer from astrocytes to oligodendrocytes was also increased after hypoxia. As increased exogenous cholesterol was seen to increase oligodendrocyte maturation, increased cholesterol synthesis by astrocytes could serve a potential neuroprotective role in hypoxic brain injury.

CRediT authorship contribution statement

Vadanya Shrivastava: Writing – original draft, Visualization, Validation, Methodology, Investigation, Formal analysis, Data curation, Conceptualization. **Sagar Tyagi:** Writing – review & editing, Validation, Methodology, Investigation. **Devanjan Dey:** Writing – review & editing, Methodology, Formal analysis. **Archna Singh:** Writing – review & editing, Validation, Methodology, Conceptualization. **Jayanth Kumar Palanichamy:** Writing – review & editing, Validation, Supervision, Conceptualization. **Subrata Sinha:** Writing – review & editing, Conceptualization. **J.B. Sharma:** Writing – review & editing, Supervision, Project administration, Methodology, Investigation. **Pankaj Seth:** Writing – review & editing, Validation, Supervision, Resources, Project administration, Methodology, Funding acquisition, Conceptualization. **Sudip Sen:** Writing – review & editing, Validation, Supervision, Resources, Project administration, Funding acquisition, Conceptualization.

Declaration of competing interest

The authors have no relevant financial or nonfinancial interests to disclose.

Data availability

Transcriptomic data has been submitted to SRA database (repository).

Acknowledgements

The authors are grateful to Department of Biotechnology (Grant number: BT/PR21413/MED/122/40/2016) and Department of Health Research (Grant number: 2022-1295), Government of India for funding this research.

Appendix A. Supplementary data

Supplementary data to this article can be found online at <https://doi.org/10.1016/j.bbadi.2024.167476>.

References

- [1] S. Kuhn, L. Gritti, D. Crooks, Y. Dombrowski, Oligodendrocytes in development, myelin generation and beyond, *Cells* 8 (11) (2019) 1424, <https://doi.org/10.3390/cells8111424>.
- [2] M. Motavaf, X. Piao, Oligodendrocyte development and implication in perinatal white matter injury, *Front. Cell. Neurosci.* 4 (15) (2021) 764486, <https://doi.org/10.3389/fncel.2021.764486>.
- [3] M.V. Sofroniew, H.V. Vinters, Astrocytes: biology and pathology, *Acta Neuropathol.* 119 (1) (2010) 7–35, <https://doi.org/10.1007/s00401-009-0619-8>.
- [4] H.S. Domingues, C.C. Portugal, R. Socodato, J.B. Relvas, Oligodendrocyte, astrocyte, and microglia crosstalk in myelin development, damage, and repair, *Front. Cell Dev. Biol.* 28 (4) (2016) 71, <https://doi.org/10.3389/fcell.2016.00071>.
- [5] H. Kray, S.L. Lindsay, S. Hosseinzadeh, S.C. Barnett, The multifaceted role of astrocytes in regulating myelination, *Exp. Neurol.* 283 (Pt B) (2016) 541–549, <https://doi.org/10.1016/j.exenneuro.2016.03.009>.
- [6] V. Shrivastava, D. Dey, C.M.S. Singal, P. Jaiswal, A. Singh, J.B. Sharma, P. Chattopadhyay, N.R. Nayak, J.K. Palanichamy, S. Sinha, P. Seth, S. Sen, Glutamate uptake is not impaired by hypoxia in a culture model of human fetal neural stem cell-derived astrocytes, *Genes (Basel)* 13 (3) (2022) 506, <https://doi.org/10.3390/genes13030506>.
- [7] C. Kose, S. Uslu, D. Calik-Kocaturk, B. Ozdil, H. Aktug, JNK inhibition modulates the cytoskeleton, hypoxia, and neurogenesis on the protein level in glioblastoma cells and astrocytes: an immunofluorescence study, *Turk. Neurosurg.* 33 (6) (2023) 982–989, <https://doi.org/10.5137/1019-5149.JTN.38289-22.1>.
- [8] O. Osemwogie, L. Butler, S. Subbiah, E. Smith, Effects of in vitro exposure of perfluorooctanoic acid and monocrotaphos on astroglioma SVG p12 cells, *J. Appl. Toxicol.* 41 (9) (2021) 1380–1389, <https://doi.org/10.1002/jat.4129>.
- [9] D. Dey, S. Tyagi, V. Shrivastava, S. Rani, J.B. Sharma, S. Sinha, J.K. Palanichamy, P. Seth, S. Sen, Using human fetal neural stem cells to elucidate the role of the JAK-STAT cell signaling pathway in oligodendrocyte differentiation in vitro, *Mol. Neurobiol.* (2024), <https://doi.org/10.1007/s12035-024-03928-9>.
- [10] S.A. Back, B.H. Han, N.L. Luo, C.A. Chricton, S. Xanthoudakis, J. Tam, K.L. Arvin, D.M. Holtzman, Selective vulnerability of late oligodendrocyte progenitors to hypoxia-ischemia, *J. Neurosci.* 22 (2) (2002) 455–463, <https://doi.org/10.1523/JNEUROSCI.22-02-00455.2002>.
- [11] N. Yates, A.J. Gunn, L. Bennet, S.K. Dhillon, J.O. Davidson, Preventing brain injury in the preterm infant-current controversies and potential therapies, *Int. J. Mol. Sci.* 22 (4) (2021) 1671, <https://doi.org/10.3390/ijms22041671>.
- [12] E. Traiffort, A. Kassoussi, A. Zahaf, Y. Laouarem, Astrocytes and microglia as major players of myelin production in normal and pathological conditions, *Front. Cell. Neurosci.* 7 (14) (2020) 79, <https://doi.org/10.3389/fncel.2020.00079>.
- [13] E.E. Benarroch, Brain cholesterol metabolism and neurologic disease, *Neurology* 71 (17) (2008) 1368–1373, <https://doi.org/10.1212/01.wnl.000033215.93440.36>.
- [14] G. Saher, S.K. Stumpf, Cholesterol in myelin biogenesis and hypomyelinating disorders, *Biochim. Biophys. Acta* 1851 (8) (2015) 1083–1094, <https://doi.org/10.1016/j.bbapap.2015.02.010>.
- [15] T. Smolić, P. Tavčar, A. Horvat, U. Černe, A. Halužan Vasle, L. Tratnjek, M.E. Kreft, N. Scholz, M. Matis, T. Petan, R. Zorec, N. Vardjan, Astrocytes in stress accumulate lipid droplets, *Glia* 69 (6) (2021) 1540–1562, <https://doi.org/10.1002/glia.23978>.
- [16] F. Boscia, C. D'Avanzo, A. Pannaccione, A. Secondo, A. Casamassa, L. Formisano, N. Guida, S. Sokolow, A. Herchuelz, L. Annunziato, Silencing or knocking out the $\text{Na}^+/\text{Ca}^{2+}$ exchanger-3 (NCX3) impairs oligodendrocyte differentiation, *Cell Death Differ.* 20 (1) (2013) 184, doi:10.1038/cdd.2012.139. Epub 2012 Dec 10. Erratum for: doi:10.1038/cdd.2011.
- [17] A. Glowacka, E. Kilańczyk, M. Maksymowicz, M. Zawadzka, W. Leśniak, A. Filipiak, RNA-Seq transcriptome analysis of differentiated human Oligodendrocytic MO3.13 cells shows upregulation of genes involved in Myogenesis, *Int. J. Mol. Sci.* 23 (11) (2022) 5969, <https://doi.org/10.3390/ijms23115969>.
- [18] F. Lu, J. Zhu, S. Guo, B.J. Wong, F.F. Chehab, D.M. Ferriero, X. Jiang, Upregulation of cholesterol 24-hydroxylase following hypoxia-ischemia in neonatal mouse brain, *Pediatr. Res.* 83 (6) (2018) 1218–1227, <https://doi.org/10.1038/pr.2018.49>.
- [19] Z. Yu, S. Li, S.H. Lv, H. Piao, Y.H. Zhang, Y.M. Zhang, H. Ma, J. Zhang, C.K. Sun, A. P. Li, Hypoxia-ischemia brain damage disrupts brain cholesterol homeostasis in neonatal rats, *Neuropediatrics* 40 (4) (2009) 179–185, <https://doi.org/10.1055/s-0029-1243175>.
- [20] N. Camargo, A. Goudriaan, A.F. van Deijk, W.M. Otte, J.F. Brouwers, H. Lodder, D. H. Gutmann, K.A. Nave, R.M. Dijkhuizen, H.D. Mansvelder, R. Chrast, A.B. Smit, M.H.G. Verheijen, Oligodendroglial myelination requires astrocyte-derived lipids, *PLoS Biol.* 15 (5) (2017) e1002605, <https://doi.org/10.1371/journal.pbio.1002605>.
- [21] Y. Xie, X. Zhang, P. Xu, N. Zhao, Y. Zhao, Y. Li, Y. Hong, M. Peng, K. Yuan, T. Wan, R. Sun, D. Chen, L. Xu, J. Chen, H. Guo, W. Shan, J. Li, R. Li, Y. Xiong, D. Liu, Y. Wang, G. Liu, R. Ye, X. Liu, Aberrant oligodendroglial LDL receptor orchestrates demyelination in chronic cerebral ischemia, *J. Clin. Invest.* 131 (1) (2021) e128114, <https://doi.org/10.1172/JCI128114>.
- [22] E.S. Mathews, B. Appel, Cholesterol biosynthesis supports myelin gene expression and axon ensheathment through modulation of PI3K/Akt/mTor signaling, *J. Neurosci.* 36 (29) (2016) 7628–7639, <https://doi.org/10.1523/JNEUROSCI.0726-16.2016>.
- [23] T. Yu, A.P. Lieberman, Npc1 acting in neurons and glia is essential for the formation and maintenance of CNS myelin, *PLoS Genet.* 9 (4) (2013) e1003462, <https://doi.org/10.1371/journal.pgen.1003462>.